Journal of Electronic Materials (2022) 51:6305–6309
https://doi.org/10.1007/s11664-022-09844-9

ORIGINAL RESEARCH ARTICLE

Superconductivity and Weak Anti-localization at $KTaO_3$ (111) Interfaces

Athby H. Al-Tawhid[1] · Jesse Kanter[2] · Mehdi Hatefipour[2] · Divine P. Kumah[3] · Javad Shabani[2] · Kaveh Ahadi[1,3]

Received: 29 March 2022 / Accepted: 21 July 2022 / Published online: 19 August 2022

Abstract

The intersection of two-dimensional superconductivity and topologically nontrivial states hosts a wide range of quantum phenomena, including Majorana fermions. We report on the observation of two-dimensional superconductivity and weak anti-localization at the $TiO_x/KTaO_3$ (111) interfaces. A remnant, saturating resistance persists below the transition temperature as superconducting puddles fail to reach phase coherence. Signatures of weak anti-localization are observed near the superconducting transition, suggesting the coexistence of superconducting fluctuations and quantum coherent quasiparticle effects. The superconducting interfaces show roughly one order of magnitude larger weak anti-localization correction, compared to non-superconducting interfaces, alluding to a relatively large coherence length in these interfaces.

Keywords 2D superconductivity · weak anti-localization · $KTaO_3$

Introduction

A combination of broken inversion symmetry and strong spin–orbit coupling in two-dimensional (2D) superconductors gives rise to mixed-parity superconductivity,[1] topological Weyl superconductivity,[2] a superconducting diode effect,[3] and an upper critical field exceeding the Pauli–Chandrasekhar–Clogston limit.[4,5] 2D weak anti-localization has been used to probe surface states in topologically nontrivial systems.[6,7] The recent discovery of 2D superconductivity[8] and predictions of topologically nontrivial states[9] at the $KTaO_3$ (111) surface makes this material system a candidate platform for the coexistence of topologically nontrivial electronic states and unconventional superconductivity.

$KTaO_3$ is an incipient ferroelectric,[10] in which superconductivity emerges at low temperatures in heavily doped samples.[11] A robust 2D electron system is reported at the interfaces of $KTaO_3$ with $LaTiO_3$,[12] $LaVO_3$,[13] EuO,[14] $LaAlO_3$,[15] TiO_x[16] and $LaCrO_3$.[16] The $KTaO_3$ conduction states are derived from Ta 5*d* and have a smaller effective mass and higher mobility and spin–orbit coupling compared to Ti 3*d* states in $SrTiO_3$.[17,18] Spin–orbit coupling lifts the degeneracy of the Ta 5*d* states and splits them into $J = 3/2$ and $J = ½$ with a 0.4-eV energy gap, where J is the total angular momentum.[19] Recently, an exotic 2D superconductivity was discovered at the (111)[8] and (110)[20] $KTaO_3$ interfaces with EuO and $LaAlO_3$, which shows nearly two orders of magnitude enhancement in the critical temperature of superconductivity (T_C) compared to its 3D counterpart.[11] Interestingly, $KTaO_3$ (100) interfaces do not show a superconducting transition. The superconducting state in the $KTaO_3$ (111) surface is highly susceptible to the interfacial structure, and a remnant resistance is observed below the superconducting transition temperature.[21] This failed superconductor state[22] is an ideal platform for the experimental realization of simultaneous superconductivity and nontrivial topology.

Here, we report on the observation of a superconducting transition at the $TiO_x/KTaO_3$(111) interfaces. A true superconducting ground state ($Rs = 0$), however, does not emerge as the superconducting puddles fail to reach phase coherence. Signatures of weak anti-localization are observed below the superconducting transition temperature, suggesting the coexistence of superconductivity and topologically nontrivial states at the $KTaO_3$ (111) surfaces.

✉ Kaveh Ahadi
kahadi@ncsu.edu

1 Department of Materials Science and Engineering, North Carolina State University, Raleigh, NC 27695, USA

2 Center for Quantum Phenomena, Department of Physics, New York University, New York 10003, USA

3 Department of Physics, North Carolina State University, Raleigh, NC 27695, USA

Materials and Methods

Mobile carriers were introduced to the (111) surface of the $KTaO_3$ single crystals using a 3-nm TiO_x layer which induces oxygen vacancies. Here, the TiO_x layer acts as an oxygen getter and is grown using an oxide molecular beam epitaxy system with 2×10^{-10} Torr base pressure. An ultra-high purity Ti source from a high-temperature effusion cell (Veeco) was used to grow a TiO_x layer. The substrate temperature was kept at 400°C during growth to create an abrupt interface. Recently, atomically abrupt interfaces were demonstrated on $KTaO_3$ interfaces grown at 600°C using an EELS map.[23] The Ti adatoms leach oxygen from $KTaO_3$, forming a TiO_x layer, and donating itinerant charge carriers to a Ta 5*d*-derived conduction band in $KTaO_3$. The reflection high-energy electron diffraction, measured during deposition, confirms the growth of an amorphous TiO_x on the (111) $KTaO_3$ surface (Supplementary materials, S1). Magneto-transport measurements were performed using the Van der Pauw configuration, and gold contacts were deposited using a sputter system at the corners of the samples through a shadow mask. The temperature-dependent magneto-transport measurements were carried out in a Quantum Design physical property measurement system with a lock-in amplifier (SR830; Stanford Research Systems) in AC mode with an excitation current of 10 μA and a frequency of 13.33 Hz. Sub-Kelvin magneto-transport measurements were carried out in a Triton dilution refrigerator (Oxford Instruments).

Oxygen vacancies introduce itinerant electrons to the Ta 5*d*-derived surface states. The conduction electrons at the low-temperature limit are derived from $J = 3/2$, Ta 5*d* states due to the large spin–orbit coupling gap in $KTaO_3$ (0.4 eV)[17,19]. Figure 1(a) shows a metallic behavior, $dR/dT > 0$, in sheet resistance with the temperature extending from room temperature to ~ 15 K. Here, oxygen stoichiometry plays an important role in transport phenomena. The oxygen vacancies donate itinerant charge carriers to the $KTaO_3$ conduction band and, similar to other point defects,[24] scatter itinerant carriers.[25] The transport in TiO_x, however, is negligible, since this layer is only 3 nm and expected to have low mobility. The sheet resistance changes somewhat linearly with temperature in this range. A resistance upturn emerges below 15 K, followed by a sharp drop below 3 K (Fig. 1(b)). The abrupt drop in sheet resistance is consistent with recently discovered 2D superconductivity at the (111) $KTaO_3$ interface.[8] Hall measurements were performed to determine the sheet carrier density. The Hall carrier density, $n = -1/(eR_H)$, where R_H is the Hall coefficient and e is the elementary charge. The Hall coefficient, $R_H = dR_{xy}/dB$, is extracted from a linear fit to the transverse resistance shown in Fig. 1c. The sheet carrier density is ~ 1×10^{14} cm^{-2} at 3 K. This carrier density is consistent with optimal doping for the critical temperature of superconductivity in (111) $KTaO_3$ interfaces.[8]

Results and Discussion

The residual resistivity ratio $\left(\rho_{300K}/\rho_{2K}\right)$ is 2.3 and the carrier mobility increases from ~ 8 cm^2/Vs at room temperature to ~ 19 cm^2/Vs at 3 K. The moderate enhancement of the carrier mobility, despite the screening of the longitudinal optical phonons at low temperatures, can be explained by the interfacial scattering of itinerant electrons.[26–28] The spatial distribution of "two-dimensional" charge carriers controls their exposure to the interfacial structure and, as a result, the mean free path of charge carriers. Here, despite the modest low-temperature carrier mobility, the sheet resistance remains below the 2D Mott–Ioffe–Regel limit (~ 20 kΩ/□). Figure 1b shows a growing positive magnetoresistance with decreasing temperature (10–2 K). The positive magnetoresistance, particularly above 4 K, cannot be explained by the emergence of superconductivity alone, and could be partially due to the weak anti-localization correction to the

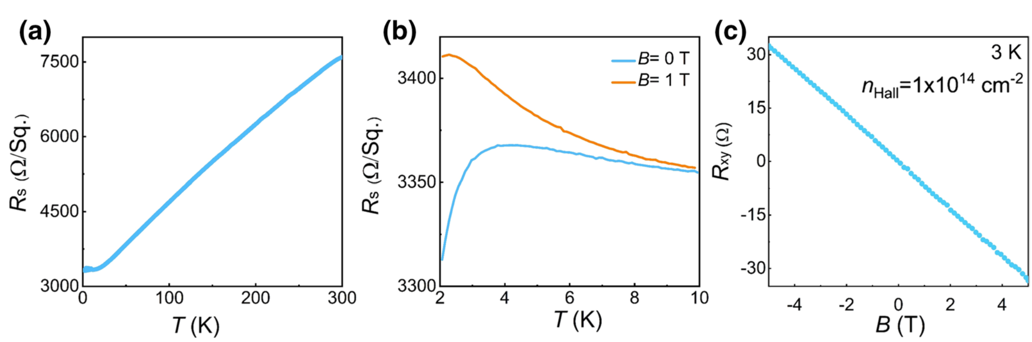

Fig. 1 Normal state electronic transport at the $TiO_x/KTaO_3(111)$ interfaces. (a) Sheet resistance with temperature (300–2 K) showing a linear scaling. (b) Magnetic field dependence of the sheet resistance–temperature behavior (10–2 K). (c) Transverse magnetoresistance at 3 K, resolving the 2D carrier density (~ 1×10^{14} cm^{-2})

longitudinal resistance. 2D electron systems at the surface of the $KTaO_3$ show large coherence length and signatures of weak anti-localization.[16,25,29,30]

Figure 2a shows the normalized resistance with temperature from 20 to 0.1 K. The resistance at 2 K and the zero field was used as normal state resistance (R_N) in Fig. 2. The sharp drop in resistance is consistent with the observed superconducting transition at the interfaces of (111) $KTaO_3$ with EuO and $LAlO_3$.[8] A remnant resistance, however, is observed below the superconducting transition temperature (mid-point T_C ~ 1.1 K). The sheet resistance saturates to a nonzero value below the transition temperature, which is insensitive to the presence of cryo-filters, excluding the possibility of radiation thermalization. Furthermore, the $KTaO_3$(111)/$LaCrO_3$ interfaces, in which the normal state resistance is above the 2D Mott–Ioffe–Regel limit (~ 33 kΩ/☐ at 3 K), do not show an abrupt drop in sheet resistance (Supplementary information, S2). Recently, a gate tunable remnant resistance was reported at the $KTaO_3$(111)/$LaAlO_3$ interfaces below the superconducting transition temperature,[21] highlighting the role of interfacial structure on the emergence of a true superconducting ground state (Rs = 0). A residual resistance has been observed in a wide range of 2D superconductors.[31–34] Here, the remnant resistance below the superconducting transition provides a unique platform for the experimental realization of 2D superconducting fluctuations coexisting with weak anti-localization.

The normalized longitudinal magnetoresistance shows that the relative change of resistance with the magnetic field ($R_{5T} - R_{0T}/R_{0T} = 0.24, at0.3K$) is large compared to the resistance change with temperature ($R_{3K} - R_{0.3K}/R_{0.3K} = 0.198, at0T$), alluding to the presence of both pair formation/breaking and weak anti-localization corrections in sheet resistance below the transition temperature.[35] Furthermore, a sharp change in the resistance with the magnetic field is observed at low field (inset in Fig. 2), consistent with the weak anti-localization.[36] The low field magneto-conduction, however, could not be explained by the Hikami–Larkin–Nagaoka model[37] due to the mixed weak anti-localization and superconducting corrections (Supplementary materials, S3).

The angle-dependent longitudinal magnetoresistance was measured to confirm the presence of the weak anti-localization effect. Figure 3a shows a transition from linear positive magnetoresistance to a parabolic behavior, with rotating the magnetic field from out-of-plane (90°) to in-plane (0°), respectively, suggesting a 2D weak anti-localization correction. To parse out the superconducting and weak anti-localization components, the longitudinal magnetoresistance was measured and compared between superconducting, $KTaO_3$ (111), and non-superconducting, $KTaO_3$ (100), interfaces (Fig. 3b). Both interfaces show a positive and linear magnetoresistance with the out-of-plane magnetic field. The superconducting interface, however, shows stronger weak anti-localization correction to resistance. The large magnetoresistance at (111) interfaces could also be explained by the pre-formed Cooper pairs.[35] The in-plane magnetoresistance of the superconducting interface shows only 1% positive magnetoresistance at 3 K and 5 T, suggesting that the pair-breaking correction could not explain the large positive magnetoresistance at the superconducting interfaces.

To briefly summarize the results, our main findings are as follows: (1) TiO_x/$KTaO_3$(111) interfaces show an abrupt superconducting transition; (2) The superconducting transition is sensitive to the normal state resistance and a nonzero, saturating resistance persists below the transition temperature; and (3) superconducting transition emerges near weak anti-localization, suggesting that superconducting fluctuations coexist with quantum coherent quasiparticle effects.

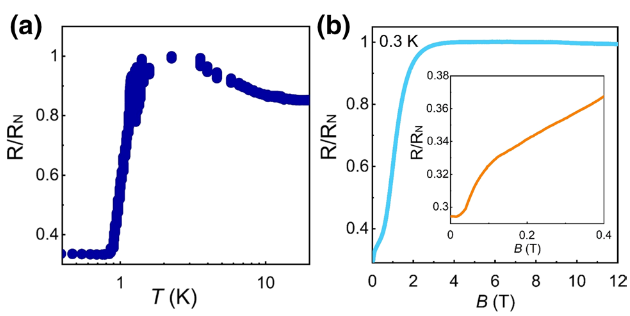

Fig. 2 Superconducting transition at the TiO_x/$KTaO_3$(111) interfaces. (a) Superconducting transition with temperature (mid-point T_C ~ 1.1 K); a remnant, saturating resistance is observed below the superconducting transition temperature. (b) Longitudinal magnetoresistance shows the superconducting transition and low field signatures of weak anti-localization (inset) at 0.3 K; the resistance at 2 K and the zero field was used as normal state resistance ®$_N$)

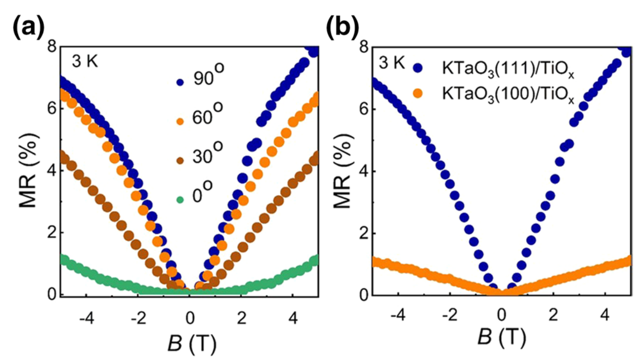

Fig. 3 Weak anti-localization at the TiO_x/$KTaO_3$ interfaces. (a) Angle-dependent magnetoresistance at the TiO_x/$KTaO_3$(111) interface; the transition from positive linear (out-of-plane field) to parabolic (in-plane field) suggests a 2D weak anti-localization. (b) Out-of-plane (90°) magnetoresistance shows weak anti-localization in superconducting, (111), and non-superconducting, (100), TiO_x/$KTaO_3$ interfaces

The first important conclusion from these results is that the emergence of superconductivity at the $KTaO_3$ interfaces depends strongly on the interfacial structure. Here, interfacial defects, microstructure, and inhomogeneity could suppress superconducting order parameters, and give rise to a remnant resistance below the transition temperature. $KTaO_3$, unlike $SrTiO_3$, does not experience structural instability and remains cubic at low temperature.[17,38] This excludes structural domains[39–41] as the source of the observed superconducting behavior. Here, the transition could be sensitive to the relaxation time of charge carriers, as the interfaces with sheet resistance above the Mott–Ioffe—Regel limit ($h/\tau \sim E_F$, where h, τ, and E_F are Planck's constant, relaxation rate, and Fermi energy, respectively) do not show a superconducting transition. This is consistent with a recent report demonstrating electric field control of a superconductor–insulator transition at the $LaAlO_3/KTaO_3$ (111) interface.[21] Alternatively, the inhomogeneity of TiO_x layer could create an inhomogeneous 2D electron system and superconductivity. The observation of a remnant resistance below the transition temperature means that the superconducting puddles form, but fail to coalesce or reach a global phase coherence mediated by Josephson coupling.[32,42–44] Here, the fluctuations of superconducting order parameter in different puddles could limit the long-range phase coupling.[32]

Next, we discuss the observation of weak anti-localization near superconducting transition. 2D electron systems at the $KTaO_3$ interfaces show signatures of weak anti-localization.[16,29,30] Furthermore, topologically nontrivial states are predicted at the $KTaO_3$ (111) surface.[9] The observed weak anti-localization correction, however, is present in both (111) and (100) interfaces. The large weak anti-localization, i.e., the coherence length, at the (111) interface could be due to the topologically nontrivial states.[7] Resolving the topological nature of surface electronic states, however, requires further study. The 2D Hikami–Larkin–Nagaoka model[37] does not describe the low-field magneto-conduction behavior at 30 mK, due to the mixed superconducting and weak anti-localization corrections (Supplementary materials, S3). The $KTaO_3$ samples are air-sensitive, and exposure to ambient oxygen fills the surface vacancies, and the 2DEG carrier density declines with exposure to ambient or oxygen annealing.[16] We observe a similar carrier density drop and suppression of the superconductivity in samples without a capping layer, due to the strong dependence of superconductivity to carrier density (Supplementary materials, S4). Interestingly, these samples show a linear positive magnetoresistance, after the demise of superconductivity, which could be explained by a 2D Hikami–Larkin–Nagaoka fit, with a resolved coherence length of 103 nm (Supplementary materials, S5), consistent with a previous report.[30]

In summary, our results, especially the coexistence of superconducting fluctuations and quantum coherent quasiparticle effects, should be of interest for the experimental realization of non-abelian excitations in a single material. We stress that our findings warrant further study of the topological nature of surface states in $KTaO_3$ (111) and the coexistence of topologically nontrivial states with superconductivity.

Supplementary Information The online version contains supplementary material available at https://doi.org/10.1007/s11664-022-09844-9.

Acknowledgements K.A. thanks Anand Bhattacharya. NC team was supported by the U.S. National Science Foundation under Grant No. NSF DMR-1751455. NYU team acknowledges funding from U.S. National Science Foundation award no. 2137776.

Data Availability The data that support the findings of this study are available within the article.

Declarations

Conflict of interests The authors declare that they have no conflict of interest.

References

1. S. Hoshino, R. Wakatsuki, K. Hamamoto, and N. Nagaosa, *Phys. Rev. B* 98, 054510 (2018).
2. S. Kanasugi, and Y. Yanase, *Phys. Rev. B* 100, 094504 (2019).
3. F. Ando, Y. Miyasaka, T. Li, J. Ishizuka, T. Arakawa, Y. Shiota, T. Moriyama, Y. Yanase, and T. Ono, *Nature* 584, 373 (2020).
4. S. Kanasugi, and Y. Yanase, *Phys. Rev. B* 98, 024521 (2018).
5. T. Schumann, L. Galletti, H. Jeong, K. Ahadi, W.M. Strickland, S. Salmani-Rezaie, and S. Stemmer, *Phys. Rev. B* 101, 100503 (2020).
6. G.M. Stephen, O.A. Vail, J. Lu, W.A. Beck, P.J. Taylor, and A.L. Friedman, *Sci. Rep.* 10, 1–7 (2020).
7. L. Bao, L. He, N. Meyer, X. Kou, P. Zhang, Z. Chen, A.V. Fedorov, J. Zou, T.M. Riedemann, T.A. Lograsso, K.L. Wang, G. Tuttle, and F. Xiu, *Sci. Rep.* 2, 1–7 (2012).
8. C. Liu, X. Yan, D. Jin, Y. Ma, H.-W. Hsiao, Y. Lin, T.M. Bretz-Sullivan, X. Zhou, J. Pearson, B. Fisher, J.S. Jiang, W. Han, J.-M. Zuo, J. Wen, D.D. Fong, J. Sun, H. Zhou, and A. Bhattacharya, *Science* 371, 716–721 (2021).
9. C. Bareille, F. Fortuna, T.C. Rödel, F. Bertran, M. Gabay, O.H. Cubelos, A. Taleb-Ibrahimi, P. Le Fèvre, M. Bibes, A. Barthélémy, T. Maroutian, P. Lecoeur, M.J. Rozenberg, and A.F. Santander-Syro, *Sci. Rep.* 4, 1–5 (2014).
10. A.R. Akbarzadeh, L. Bellaiche, K. Leung, J. Íñiguez, and D. Vanderbilt, *Phys. Rev. B* 70, 054103 (2004).
11. K. Ueno, S. Nakamura, H. Shimotani, H.T. Yuan, N. Kimura, T. Nojima, H. Aoki, Y. Iwasa, and M. Kawasaki, *Nat. Nanotechnol.* 6, 408 (2011).
12. K. Zou, S. Ismail-Beigi, K. Kisslinger, X. Shen, D. Su, F.J. Walker, and C.H. Ahn, *APL Mater.* 3, 036104 (2015).
13. S. Goyal, N. Wadehra, and S. Chakraverty, *Adv. Mater. Interfaces* 7, 2000646 (2020).
14. H. Zhang, Y. Yun, X. Zhang, H. Zhang, Y. Ma, X. Yan, F. Wang, G. Li, R. Li, T. Khan, Y. Chen, W. Liu, F. Hu, B. Liu, B. Shen, W. Han, and J. Sun, *Phys. Rev. Lett.* 121, 116803 (2018).

15. H. Zhang, H. Zhang, X. Yan, X. Zhang, Q. Zhang, J. Zhang, F. Han, L. Gu, B. Liu, Y. Chen, B. Shen, J. Sun, and A.C.S. Appl, *Mater. Interfaces* 9, 36456 (2017).
16. A.H. Al-Tawhid, D.P. Kumah, and K. Ahadi, *Appl. Phys. Lett.* 118, 192905 (2021).
17. B. Himmetoglu, and A. Janotti, *J. Phys. Condens. Matter* 28, 065502 (2016).
18. V.R. Cooper, *Phys. Rev. B* 85, 235109 (2012).
19. F.Y. Bruno, S. McKeown Walker, S. Riccò, A. de la Torre, Z. Wang, A. Tamai, T.K. Kim, M. Hoesch, M.S. Bahramy, and F. Baumberger (2019) Adv Electron Mater, 5:1800860
20. Z. Chen, Z. Liu, Y. Sun, X. Chen, Y. Liu, H. Zhang, H. Li, M. Zhang, S. Hong, T. Ren, C. Zhang, H. Tian, Y. Zhou, J. Sun, and Y. Xie, *Phys. Rev. Lett.* 126, 026802 (2021).
21. Z. Chen, Y. Liu, H. Zhang, Z. Liu, H. Tian, Y. Sun, M. Zhang, Y. Zhou, J. Sun, and Y. Xie, Science (80), 372, 721 (2021).
22. A. Kapitulnik, S.A. Kivelson, and B. Spivak, *Rev. Mod. Phys.* 91, 011002 (2019).
23. S. Mallik, G. Ménard, G. Saïz, H. Witt, J. Lesueur, A. Gloter, L. Benfatto, M. Bibes, and N. Bergeal, (2022), arXiv:2204.09094
24. S. Salmani-Rezaie, H. Kim, K. Ahadi, and S. Stemmer, *Phys. Rev. Mater.* 3, 114404 (2019).
25. A.H. Al-Tawhid, J. Kanter, M. Hatefipour, D.L. Irving, D.P. Kumah, J. Shabani, and K. Ahadi, (2021), arXiv:2109.08073
26. K. Ahadi, and S. Stemmer, *Phys. Rev. Lett.* 118, 236803 (2017).
27. K. Ahadi, O.F. Shoron, P.B. Marshall, E. Mikheev, and S. Stemmer, *Appl. Phys. Lett.* 110, 062104 (2017).
28. K. Ahadi, H. Kim, and S. Stemmer, *APL Mater.* 6, 056102 (2018).
29. N. Wadehra, R. Tomar, R.M. Varma, R.K. Gopal, Y. Singh, S. Dattagupta, and S. Chakraverty, *Nat. Commun.* 11, 1 (2020).
30. H. Nakamura, and T. Kimura, *Phys. Rev.B* 80, 124021 (2009).
31. Y. Saito, Y. Kasahara, J. Ye, Y. Iwasa, and T. Nojima, *Science* 350, 409–413 (2015).
32. Z. Chen, A.G. Swartz, H. Yoon, H. Inoue, T.A. Merz, D. Lu, Y. Xie, H. Yuan, Y. Hikita, S. Raghu, and H.Y. Hwang, *Nat. Commun.* 9, 1–6 (2018).
33. C. Yang, Y. Liu, Y. Wang, L. Feng, Q. He, J. Sun, Y. Tang, C. Wu, J. Xiong, W. Zhang, X. Lin, H. Yao, H. Liu, G. Fernandes, J. Xu, J.M. Valles, J. Wang, and Y. Li, *Science* 366, 1505 (2019).
34. A.W. Tsen, B. Hunt, Y.D. Kim, Z.J. Yuan, S. Jia, R.J. Cava, J. Hone, P. Kim, C.R. Dean, and A.N. Pasupathy, *Nat. Phys* 123, 208 (2015).
35. J. Wang, W. Powers, Z. Zhang, M. Smith, B.J. McIntosh, S.-K. Bac, L. Riney, M. Zhukovskyi, T. Orlova, L.P. Rokhinson, Y.T. Hsu, X. Liu, and B.A. Assaf, (2021), arXiv:2112.01569
36. M. Dzero, M.G. Vavilov, K. Kechedzhi, and V.M. Galitski, *Phys. Rev. B* 92, 165415 (2015).
37. S. Hikami, A.I. Larkin, and Y. Nagaoka, *Prog. Theor. Phys.* 63, 707 (1980).
38. P. Grenier, G. Bernier, S. Jandl, B. Salce, and L.A. Boatner, *J. Phys. Condens. Matter* 1, 2515 (1989).
39. S. Salmani-Rezaie, K. Ahadi, W.M. Strickland, and S. Stemmer, *Phys. Rev. Lett.* 125, 087601 (2020).
40. S. Salmani-Rezaie, K. Ahadi, and S. Stemmer, *Nano Lett.* 20, 6542 (2020).
41. K. Ahadi, L. Galletti, Y. Li, S. Salmani-Rezaie, W. Wu, and S. Stemmer, *Sci. Adv.* 5, eaaw0120 (2019).
42. S. Eley, S. Gopalakrishnan, P.M. Goldbart, and N. Mason, *Nat. Phys.* 8, 59–62 (2011).
43. H.S.J. van der Zant, F.C. Fritschy, W.J. Elion, L.J. Geerligs, and J.E. Mooij, *Phys. Rev. Lett.* 69, 2971 (1992).
44. C.G.L. Bøttcher, F. Nichele, M. Kjaergaard, H.J. Suominen, J. Shabani, C.J. Palmstrøm, and C.M. Marcus, *Nat. Phys.* 1411, 1138 (2018).